IOP Conf. Series: Journal of Physics: Conf. Series **783** (2017) 012047 doi:10.1088/1742-6596/783/1/012047

# Modeling and comparative study of linear and nonlinear controllers for rotary inverted pendulum

**Byron Lima[1], Ricardo Cajo[2], Víctor Huilcapi[1], Wilton Agila[2]**

[1]Departamento de Ingeniería Electrónica, Universidad Politécnica Salesiana, Guayaquil, Ecuador, Robles 107 y Chambers, Guayaquil, Ecuador.
[2]Facultad de Ingeniería en Electricidad y Computación, Escuela Superior Politécnica del Litoral, ESPOL, Campus Gustavo Galindo Km 30.5 Vía Perimetral, P.O. Box 09-01-5863, Guayaquil, Ecuador.

Email: [1]{blimac, vhuilcapi}@ups.edu.ec, [2]{rcajo,wagila}@espol.edu.ec

**Abstract**. The rotary inverted pendulum (RIP) is a problem difficult to control, several studies have been conducted where different control techniques have been applied. Literature reports that, although problem is nonlinear, classical PID controllers presents appropriate performances when applied to the system. In this paper, a comparative study of the performances of linear and nonlinear PID structures is carried out. The control algorithms are evaluated in the RIP system, using indices of performance and power consumption, which allow the categorization of control strategies according to their performance. This article also presents the modeling system, which has been estimated some of the parameters involved in the RIP system, using computer-aided design tools (CAD) and experimental methods or techniques proposed by several authors attended. The results indicate a better performance of the nonlinear controller with an increase in the robustness and faster response than the linear controller.

## 1. Introduction

The rotary inverted pendulum is a classic problem in the control systems area, which allows to evaluate performance and demonstrate the effectiveness of control techniques. The RIP system is a simple structure with not minimum phase multivariable unstable and highly nonlinear characteristics. It has a pendulum arm attached to a rotary instead of a moving car [1]. Several works have presented some methods to modeling dynamic systems such as: the used Euler-Lagrange in [2-6] with good result, so it is used to model the dynamics of rotary inverted pendulum shown in [7]. Moreover, the mathematical modeling used with the iterative method of nonlinear least squares that uses the Trust-Region-Reflective Algorithm, which tries to minimize the error between the actual and simulated signals [8].

Research community has studied and proposed diverse improvements to the classical PID approach in RIP systems: linear PID with a direct control of each system variable [9], Fuzzy Logic focused on a fuzzy controller [10], Optimum state regulator [11], and genetic algorithm based controller (GA) [12]. All the proposed controllers referred in the articles in this paragraph aim to identify, optimize and stabilize systems in general.

The research developed in this paper proposes to apply some methods, techniques and the use of CAD tools for estimating parameters that are not easy to measure and study because of the performance of RIP system by using a nonlinear control technique (nonlinear PID) presented in [13]. This nonlinear version is based on the classical method of Ziegler and Nichols tuning in the frequency domain.

This article is organized as follows: Section 1 presents the introduction, Section 2 describes the system used. Mathematical modelling for RIP system shown in section 3, section 4 estimating some parameters of the RIP system is performed. The validation of the model with the estimated parameters is shown in Section 5.Section 6 shows the design of linear and nonlinear PID controllers. Section 7 shows the results and performance of the algorithms developed control. Finally, some conclusions are summarized in Section 8.

## 2. Description of the System

The RIP system is controlled from a PC, therefore the system contains hardware and software that can be easily installed in a laboratory. Regarding the hardware, the system consists of panel start and stop emergency button, power supply, quadrature signal decoder with Arduino Mega, engine driver Sabertooth Dual 2x32A / 6V-24V and interface to a PC through the card PCI-1711 and CB-68LP connector block as shown in Figure 1.

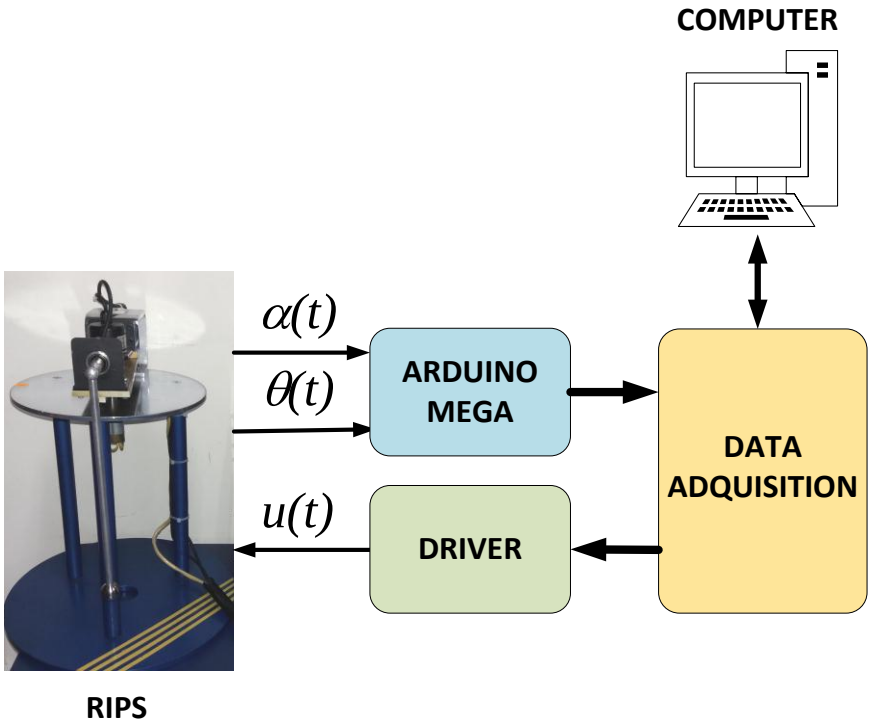


**Figure 1**. Schematic architecture of the RIP system

In order to measure the angular position of the pendulum and arm $(\alpha,\theta)$ is used an incremental encoder model E50S8-600-3-type T-24, which measures with high precision (600 pulses per revolution), and the angle and direction of rotation through phases A and B

## 3. Mathematical model

The RIP system consists of a cylindrical rod with freedom to oscillate about a fixed pivot, which is mounted on an arm following an angular movement as shown in Figure 2.

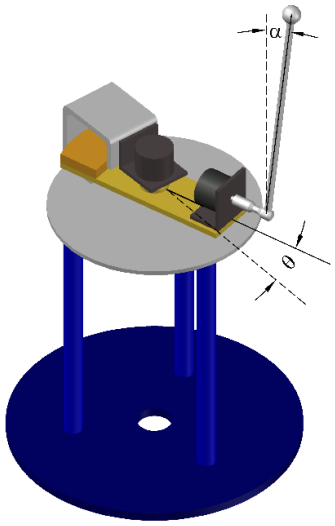


**Figure 2**. The rotary inverted pendulum system

The mathematical model for RIP system used in the present study is based in the work developed in [8], which representation is given by:

$$\begin{bmatrix} \left(J_P + m_p L^2\right) & -\left(m_p r L \cos\alpha\right) \\ -\left(m_p r L \cos\alpha\right) & \left(J_r + m_p r^2\right) \end{bmatrix} \begin{bmatrix} \ddot{\alpha} \\ \ddot{\theta} \end{bmatrix} = \begin{bmatrix} m_p g L \sin\alpha - B_p \dot{\alpha} \\ \frac{k_t}{R_a} V_a - \left(\frac{k_t k_b}{R_a} + B_r\right)\dot{\theta} - \left(m_p r L \sin\alpha\right)(\dot{\alpha})^2 \end{bmatrix} \tag{1}$$

The RIP system is described in space state as follows:

$$\begin{aligned} &\frac{d}{dt}x_1 = x_2 \\ &\frac{d}{dt}x_2 = \frac{k_t k_2 k_{DG} \cos x_1}{R_a\left(k_1 k_5 - k_2 k_4 \cos^2 x_1\right)} u - \frac{k_2 \cos x_1 \left(k_b k_t + R_a B_r\right)}{R_a\left(k_1 k_5 - k_2 k_4 \cos^2 x_1\right)} x_4 - \ldots \\ &\frac{k_2 k_6 (\sin x_1)(\cos x_1) {x_2}^2}{k_1 k_5 - k_1 k_4 \cos^2 x_1} - \frac{k_5\left(B_p x_2 - k_3 \sin x_1\right)}{k_1 k_5 - k_2 k_4 \cos^2 x_1} \\ &\frac{d}{dt}x_3 = x_4 \\ &\frac{d}{dt}x_4 = \frac{B_p x_2 - k_3 \sin x_1 + k_1\left(\frac{d}{dt}x_2\right)}{k_2 \cos x_1} \end{aligned} \tag{2}$$

The output is given by:

$$y = [x_1 \;\; x_3]^T \tag{3}$$

where,

$\alpha$: Pendulum position, $\dot{\alpha}$: Pendulum velocity, $\theta$: Arm position , $\dot{\theta}$: Arm velocity, $u$: Control signal to the motor

Each physical signal $[\alpha \ \dot{\alpha} \ \theta \ \dot{\theta}]$ in state-space RIP system model is represented by: $[x_1 \ x_2 \ x_3 \ x_4]$ respectively. Some intermediate model variables and parameters area used:

$$k_1 = J_P + m_p L^2, \ k_2 = m_p rL, \ k_3 = m_p gL, \ k_4 = m_p rL, \ k_5 = J_r + J_m + m_p r^2, \ k_6 = m_p rL, \ V_a = k_{DG} u \quad (4)$$

## 4. Parameter estimation

In this section the parameters estimation of the RIP is performed that is the reason why the system is analysed by parts, engine, driver, pendulum, and arm.

### *4.1. Parameter estimation for the engine*

To measure the motor parameters proceeds to undock the pendulum and analyse it independently. It starts with the estimation of the resistance and inductance of the motor armature, for which its terminals connected to NI ELVIS + National Instruments and at each angular position of the rotor several samples for resistance and inductance is taken. With these data it is possible to calculate an average whereby the values of $R_a$ and $L_a$ is obtained.

Then, proceed to estimate the Back-emf constant ( $k_b$ ), constant electromagnetic torque ( $k_t$ ), moment of inertia of the rotor of the motor ( $J_m$ ) and viscous friction coefficient of the motor ( $B_r$ ), for which the mechanical coupling between the motor shafts and encoder is performed. Similarly to the previous estimate the NI ELVIS II + module from National Instruments inductance and incremental encoder is used to measure angular velocity ( $\omega$ ) and the armature current ( $i_a$ ) for various input voltages to the motor ( $V_a$ ), using equation (5) Back-emf constant is estimated.

$$k_b = \frac{V_a - R_a i_a}{\omega} \quad (5)$$

In electrical machines must be a balance between electric power and mechanical power is obtained that $k_t = k_b$. To estimate the viscous friction coefficient of the engine ( $B_r$ ) is necessary to use the differential equation unloaded motor ( $T_L = 0$ ):

$$T_m = J_m \frac{d\omega}{dt} + B\omega \quad (6)$$

where $T_m = k_b i_a$ represents the engine torque. We proceed to energize the motor with a constant voltage for a time, until it reaches a constant speed, the angular acceleration disappears directly obtaining the ratio of viscous friction coefficient, by eliminating the term of the derivative of angular velocity and clearing, the viscous friction coefficient is obtained:

$$B = \frac{k_b i_a}{\omega} \quad (7)$$

Finally, it is estimated the moment of inertia of the rotor of the motor ( $J_m$ ), for which the equation (8) is used.

$$\tau = \frac{J_m}{B} \quad (8)$$

Where the constant ( $\tau$ ), is known as the constant mechanical engine, which is measured experimentally, as a third of the time between switching off the motor without load at a constant speed and braking.

### *4.2. Estimating gain driver*

To estimate the gain driver it must be found the relationship between the input voltage and output generated by the engine driver Sabertooth Dual 2x32A / 6V-24V. The different values of voltage applied to the input and the output are measured, the slope of the line obtained proves to be $K_{DG}$, as shown in Figure 3.

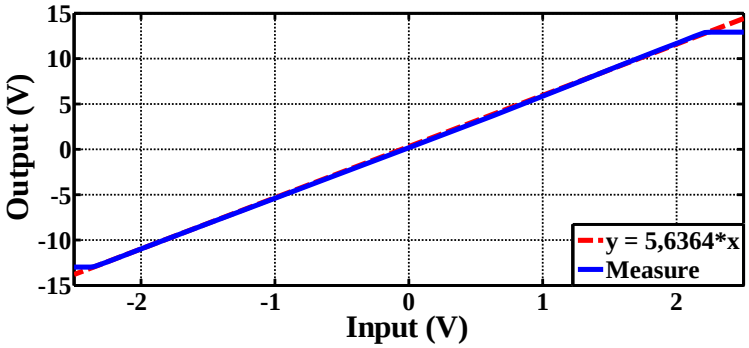


**Figure 3.** Relationship input - output driver

*4.3. Parameter estimation of the pendulum and arm*

The Pendulum mass ( $m_p$ ) is measured by an electronic precision balance, turn this value that is obtained from the CAD compared. The estimate of the length of rotation axis to the center of mass of the pendulum ( $L$ ) and the moment of inertia of the pendulum ( $J_p$ ) is also performed in CAD, for which the RIP is designed in the SolidsWorks software. For the coefficient of viscous friction in the pendulum, we proceed to measure the pendulum swing during free fall from a small height, as shown in Figure.4.

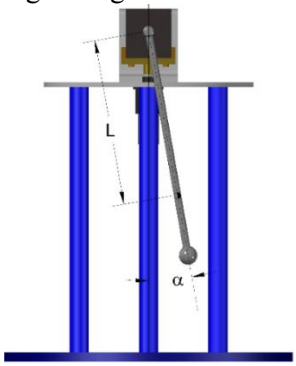


**Figure 4**. Setting the pendulum damped oscillation

The differential equation describing the oscillatory motion of the pendulum damped when it should fall from a small height, it is given by:

$$J_p \frac{d^2\alpha}{dt^2} + B_p \frac{d\alpha}{dt} + m_p g L \alpha = 0 \tag{9}$$

Where $B_p \frac{d\alpha}{dt}$ , represents the damping produced by the friction between the pendulum and air.

The solution to this equation is shown in (10):

$$\alpha = \alpha_0 e^{-B_p t / 2J_p} \cos\left(\omega_0 t + \varphi\right) \tag{10}$$

The term $\gamma = -B_p t / 2J_p$ , corresponds to the damping constant of the wobble signal of the pendulum. For this constant experimentally the pendulum is positioned with a small initial angle and drops it until it stops. The response of the pendulum and its signal envelope can be approximated as shown in Figure.5.

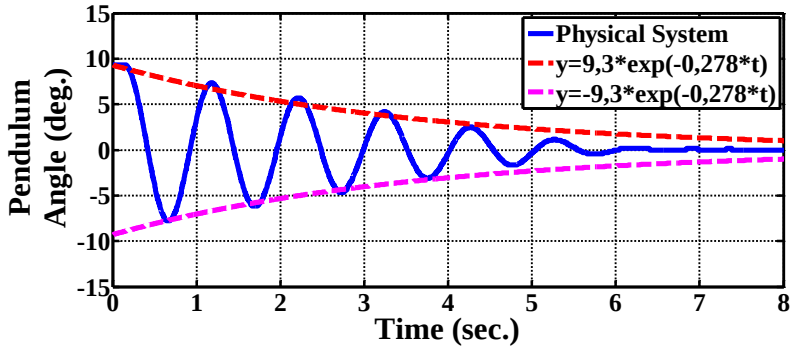


**Figure 5**. Response damped oscillatory motion of the pendulum

Finally, the estimation of the Rotating arm length ($r$) and the inertia moment arm Equivalent ( $J_r$ ) is obtained from the RIP design CAD system made previously.

## 5. Validation of the model

The estimated parameters for the RIP system experimentally, are shown in Table 1.

**Table 1.** RIP system parameters.

| Parameters | Value |
|---|---|
| $R_a$ - Armature resistance | 5.4351 Ω |
| $L_a$ - Armature inductance | 0.00188 mH |
| $k_b$ - Back-emf constant | 1.1098V.s/rad |
| $k_t$ - Constant electromagnetic torque | 1.1098 N.m/A |
| $k_{DG}$ - Gain driver | 5.6354 |
| $J_m$ -Moment of inertia of the rotor of the motor | 0.00071 kg.m$^2$ |
| $B_r$ - Viscous friction coefficient of the motor | 0.04166 N.m.s/rad |
| $g$ - Gravity acceleration | 9.8 m/seg$^2$ |
| $m_p$ -Pendulum mass | 0.13417 kg |
| $J_r$ - Equivalent inertia moment arm | 0.0078 kg.m$^2$ |
| $r$ - Rotating arm length | 0.125 m |
| $L$ - Length of rotation axis to the center of mass of the pendulum | 0.19604 m |
| $J_p$ - Moment of inertia of the pendulum | 0.001882 kg.m$^2$ |
| $B_p$ - Viscous friction coefficient of the pendulum | 4.56798.10$^{-4}$ N.m.s/rad |

The bound for control signal is set to -2.5V…+2.5V. These parameters are used in the evaluation of engine model and RIP system using MATLAB, this is discussed in section 5.1 and 5.2.

### *5.1. Evaluation of nonlinear engine model*

To validate the nonlinear engine model, is used a test signal square wave with the purpose of analyzing the dynamics of the real system and the nonlinear model.

Note that the square wave input can not be applied directly to the engine, so the engine driver Dual Sabertooth 2x32A / 6V-24V with gain $K_{DG}$ , which manages the power consumption of the motor is

used. The applied input terminals of driver and engine angular position, is shown in Figure 6. The average angular position error between the nonlinear model and the actual system is -0.0023 (deg).

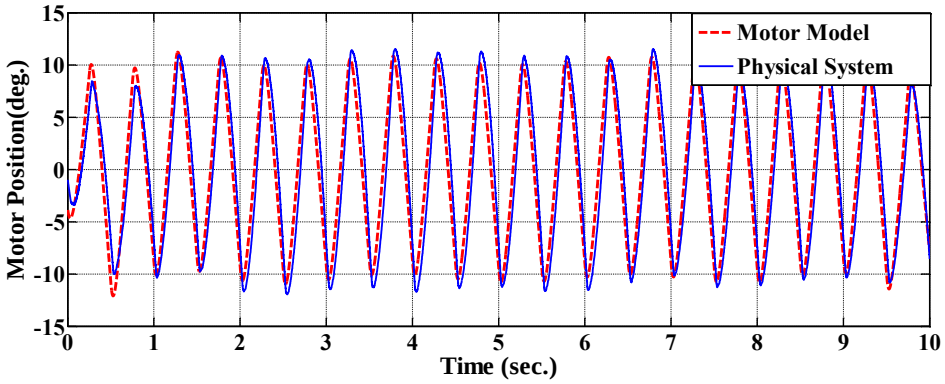


**Figure 6**. Response engine model to a square entry

*5.2. Evaluation of nonlinear system model RIP*

To validate the nonlinear model of the RIP system proceeds to generate different test signals in order to validate the estimated model. In Figure 7 is shown, the response to an input made by combining sinusoids for the position of the pendulum and the arm, which an error average angular position is obtained 1.1981 (deg) for the pendulum and -0.4431 (deg) for the arm.

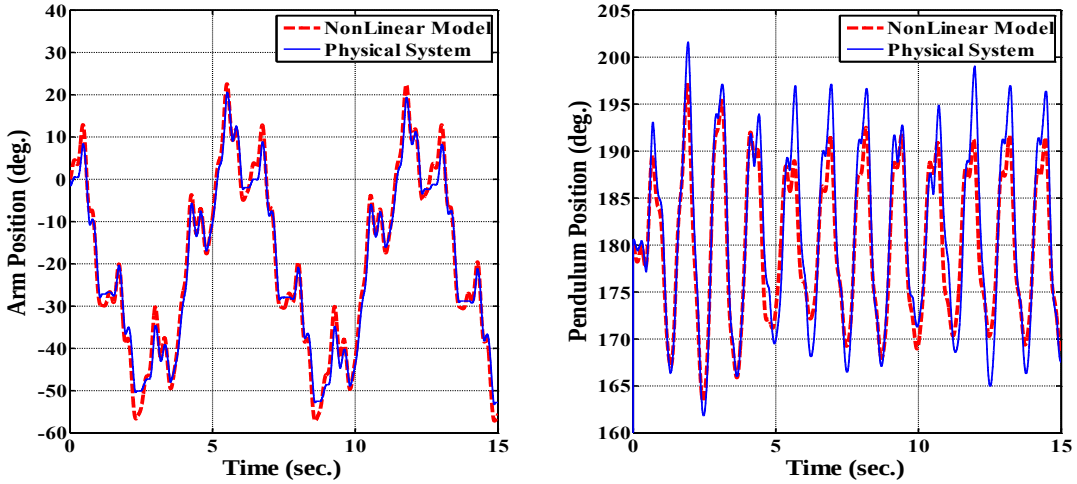


**Figure 7**. Response nonlinear model and real RIP system to an input combination of sinusoids.

## 6. PID and PI Control Algorithms Design

In this section, the development of the PID and PI controllers is carried out, the design of controllers involves the manipulation of a linear model. Thus, nonlinear RIPS model equation (1) is linearized around an equilibrium point given by the equation (11).

$$\alpha \approx 0 \ (\dot{\alpha})^2 \approx 0 \ \cos\alpha \approx 1 \ \sin\alpha \approx \alpha \tag{11}$$

Linear models are represented trough transfer functions. Transfer functions of the pendulum and arm are indicated as follows in the equations (12) and (13) respectively:

$$G_P(s) = \frac{d_5 s}{d_1 s^3 + (d_2 + d_6)s^2 + (d_3 + d_7)s + d_4 + d_8)} \tag{12}$$

$$G_A(s) = \frac{d_5(k_1 s^2 + B_p s - k_3)}{ps^4 + qs^3 + k_2(d_3 + d_7)s^2 + k_2(d_4 + d_8)s}$$
$$: d_1 = R_a(k_1 k_5 - k_4 k_2);\ \ d_2 = R_a(k_5 B_p + B_r k_1);\ \ d_3 = R_a(-k_5 k_3 + B_r B_p);\ \ d_4 = -R_a B_r k_3 \quad (13)$$
$$d_5 = k_t k_2 k_{DG};\ \ d_6 = k_b k_1 k_t;\ \ d_7 = k_b B_p k_t;\ \ d_8 = -k_b k_3 k_t;\ \ p = k_2 d_1;\ \ q = k_2 d_2 + k_2 d_6$$

*6.1. Linear PID controller for the pendulum position.*

The control structure in the case of linear PID is quite different to the classical feedback loop, this, since the control target in our study case is the vertical position of the pendulum in $\alpha = 0$ degrees, rejecting the perturbation effects as it is indicated in Figure 8.

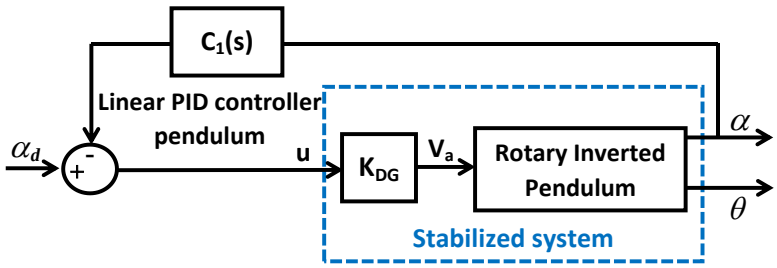


**Figure 8**. Control structure for the balance of the pendulum

The controller parameters of the PID are tuned by using SISOTOOL, which is a Matlab package. Specifically, the method utilized is LGR, the tuned controller is represented as follows: (14).

$$C_1(s) = \frac{k_{d1}s^2 + k_{p1}s + k_{i1}}{s} \quad : k_{d1} = 0.6247;\ \ k_{p1} = 25.8634;\ \ k_{i1} = 244.4404 \quad (14)$$

*6.2. Linear PID controller design for the arm position.*

The design of the pendulum controller was presented in the former section, the development of the complete control structure is presented in this section. The structure is shown in Figure 9.

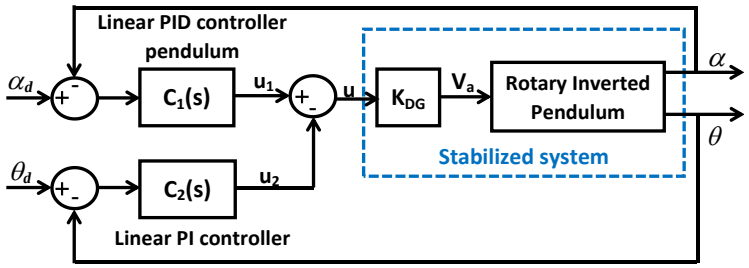


**Figure 9**. Control structure for the arm position

In the design of the linear PI arm controller, it is important to take into account that the value of $\alpha_d$ should stabilize around zero degrees, taking into account the latter, the block diagram shown in Figure 9, is reduced by using blocks algebra, the reduced block diagram leads to the following transfer function:

$$G_{2dof}(s) = -\left(\frac{k_{DG}}{1 + G_P(s)C_1(s)k_{DG}}\right)G_A(s) \quad (15)$$

As in the tunning of the former controller, the arm controller is tuned by using SISOTOOL and the LGR method. The resultant controller is given by equation (16).

$$C_2(s) = \frac{k_{p2}s + k_{i2}}{s} \quad : k_{p2} = 5.7951;\ \ k_{i2} = 5.4358 \quad (16)$$

*6.3. Nonlinear PI controller design for the arm position*

In the design of the nonlinear PI controller, it is required to linearize the RIP model given by equation (2). First, it is important to define an equilibrium point. The corresponding equilibrium point will be represented as a parametrization with respect to the input of the system, equation (17) presents the equilibrium point.

$$u = U; \quad x_1 = X_1(U) = \tan^{-1}\left(-\frac{k_t k_2 k_{DG}}{k_5 k_3 R_a} U\right); \quad x_2 = 0; \quad x_4 = 0 \tag{17}$$

The linearized model, which is represented by a state space model is presented in equation (18).

$$A_p = \begin{bmatrix} 0 & 1 & 0 & 0 \\ a & b & 0 & c \\ 0 & 0 & 0 & 1 \\ d & e & 0 & f \end{bmatrix}, \; B_p = \begin{bmatrix} 0 \\ h \\ 0 \\ i \end{bmatrix}, \; C_p = \begin{bmatrix} 1 & 0 & 0 & 0 \\ 0 & 0 & 1 & 0 \end{bmatrix}, \; D_p = 0; \quad a = \frac{(\mathrm{a}_3)^{-1/2}}{R_a a_2}\left[R_a k_3 k_5 + \frac{a_4}{R_a k_3 k_5}\right]$$

$$b = -\frac{B_p k_5}{a_2}, \quad c = -\frac{k_2 a_1}{R_a a_2}(\mathrm{a}_3)^{-1/2}, \quad h = \frac{k_2 k_t k_{DG}}{R_a b_2}(\mathrm{a}_3)^{-1/2}, \quad i = \frac{k_1 k_t k_{DG}}{R_a b_1}, \quad f = -\frac{k_1 a_1}{R_a a_2}$$

$$d = \frac{\frac{R_a k_2 k_3 {k_4}^2}{a_3} + R_a k_1 k_3 k_4 k_5 - \frac{2U^2 k_1 {k_2}^2 k_4 {k_{DG}}^2 {k_t}^2}{R_a k_3 k_5 a_3} - \frac{2R_a k_1 k_3 k_4 k_5}{a_3}}{R_a {k_1}^2 {k_5}^2 + R_a {k_2}^2 {k_4}^2 (a_3)^{-2} - 2R_a k_1 k_2 k_4 k_5 (a_3)^{-1}}, \; e = -\frac{B_p k_4}{a_2}(\mathrm{a}_3)^{-1/2} \tag{18}$$

$$a_1 = k_b k_t + B_r R_a, \qquad a_2 = k_1 k_5 - \frac{k_2 k_4}{a_3}, \qquad a_3 = \left(\frac{a_4}{R_a {}^2 k_3 {}^2 k_5 {}^2} + 1\right)$$

$$a_4 = U^2 k_2 {}^2 k_t {}^2 k_{DG} {}^2 \qquad b_1 = k_1 k_5 - \frac{k_2 k_4}{b_2}, \qquad b_2 = \left(\frac{U^2 k_2 {}^2 k_t {}^2 k_{DG} {}^2}{R_a {}^2 k_3 {}^2 k_5 {}^2} + 1\right)$$

In control theory, an alternative way of systems representation is the transfer function. Thus, equation (14) is the transfer function obtained after linearization and parametrization of the nonlinear model.

$$G_{P(U)}(s) = \frac{hs + ci - fh}{s^3 - (b+f)s^2 + (bf - a - ce)s + af - cd)}, \quad G_{A(U)}(s) = \frac{is^2 + (eh - bi)s + dh - ai}{s(s^3 - (b+f)s^2 + (bf - a - ce)s + af - cd)} \tag{19}$$

It should be noticed that the transfer function presented in equation (19) are parametrized transfer functions with respect to the input *U*. As it is indicated in section 6.2, the control scheme is the same as the one presented in Figure 9 with the difference in the transfer function *C*2(*s*) which in the present study corresponds to a nonlinear PI. With the former considerations, a reduction of the system is possible. In equation (20), a reduced version of the transfer functions is presented.

$$G_{2dof(U)}(s) = -\left(\frac{G_{A(U)}(s)}{1 + G_{P(U)}(s)C_1(s)}\right) \; : \; c_1 = i; \; c_2 = eh - bi; \; c_3 = dh - ai; \; c_4 = hk_{d1} - (b+f)$$
$$c_5 = bf - a - ce + hk_{p1} + k_{d1}(ci - fh); \quad c_6 = af - cd + hk_{i1} + k_{p1}(ci - fh); \quad c_7 = k_{i1}(ci - fh) \tag{20}$$

By using Ziegler-Nichols method, the ultimate response in frequency domain gives important information in order to obtain optimal controller parameters. Specifically, it is possible to obtain the ultimate period $P_0(\mathrm{U})$ and the ultimate gain $K_0(\mathrm{U})$. In the approach presented in this study, the ultimate gain and period are obtained based on the transfer function $G_{2dof(U)}(s)$ as follows:

$$P_0(U)=2\pi\left(\omega_0(U)\right)^{-1};\quad K_0(U)=\left|G_{2dof(U)}(j\omega_0)\right|^{-1};\quad \omega_0(U)=\left(\left(c_2c_5-c_1c_6-c_3c_4-N\right)\left(2(c_2-c_1c_4)\right)^{-1}\right)^{1/2} \tag{21}$$

$$N=\left((-c_2c_5+c_1c_6+c_3c_4)^2-4(c_2-c_1c_4)(c_2c_7-c_3c_6)\right)^{1/2};\ K_0(U)=\left|\left(\frac{(\omega^4-c_5\omega^2+c_7)^2+(c_6\omega-c_4\omega^3)^2}{(c_3-c_1\omega^2)^2+(c_2\omega)^2}\right)^{1/2}\right|$$

In the nonlinear PI controller approach considered in this study, the nonlinear controller is generalized as follows:

$$\dot{z}(t)=0.54\frac{K_0(z_v(t))}{P_0(z_v(t))}(\theta_d-x_3(t));\quad u(t)=z(t)+0.45K_0(z(t))(\theta_d-x_3(t)) \tag{22}$$

Where $z(t)$ is defined as an additional state of the nonlinear controller of the arm. The control signal $u(t)$ is associated to the $x_3(t)$ , which represents in the RIP system, the current arm position.

## 7. Performance Assessment

The values of the identified parameters are used for modeling purposes and the evaluation of the PI and PID controllers using MATLAB / Simulink, which is discussed in section 7.1 to 7.3.

### *7.1. Linear PID and PI controller evaluation*

In Figure 10 the responses of linear controllers are shown for the pendulum and arm respectively. For which different references are used as input, for a square wave arm $\pm 10$ degrees, while for the pendulum input 0 degrees is used. The Stabilization times obtained for linear controllers are: stabilization time for the pendulum $t_{SP}=0.2\,\text{sec}$ and $t_{SA}=3.25\,\text{sec}$ arm.

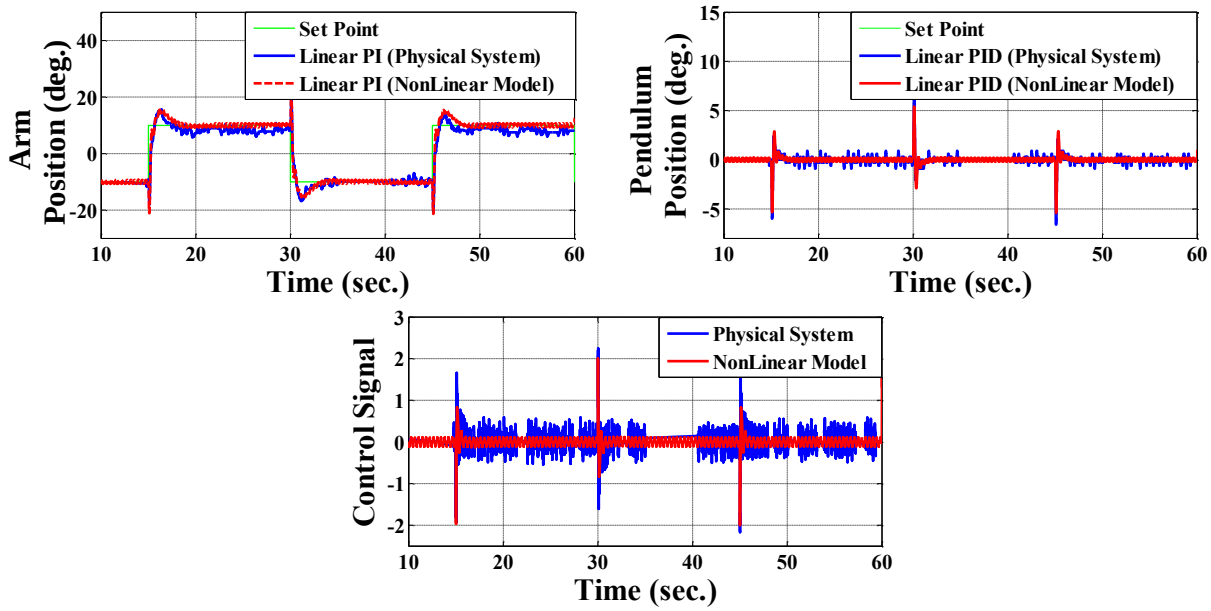


**Figure 10**. Responses of linear controllers for pendulum and arm position

### *7.2. Evaluation of the linear PID controller and nonlinear PI controller*

The input signals used in section 7.1 are again used in this section in order to evaluate the performance of the linear and nonlinear controller. The Figure 11 shows the responses of PID controllers linear and nonlinear PI with the respective control efforts. The Stabilization times obtained for the linear and nonlinear controller respectively are: stabilization time for the pendulum $t_{SP}=0.2\,\text{sec}$ and $t_{SA}=2.5\,\text{sec}$ arm.

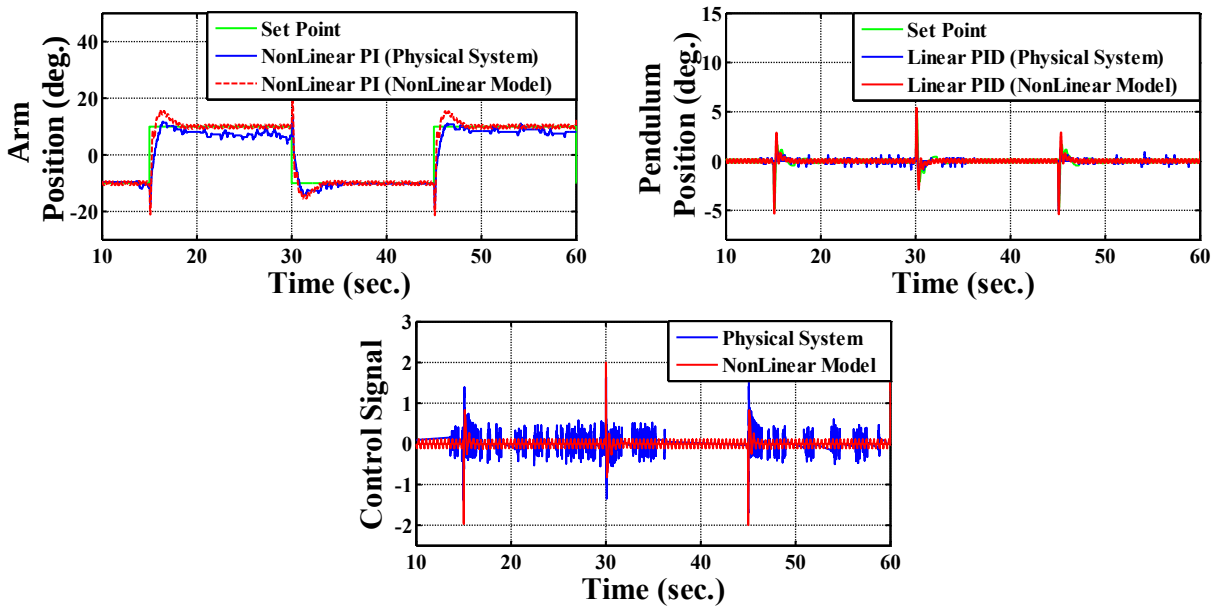


**Figure 11**. Response of linear and nonlinear controller for pendulum and arm position

*7.3. Performance Evaluation of Linear vs nonlinear controllers in the RIP system*

This section shows the results of the comparison between the linear PID controller and PI nonlinear. To carry out this performance indices such as are used: IAE (absolute integral error) and ISU (integral square control signal deviation), which will allow us to measure the cumulative error that penalizes the monitoring process and the energy used by the controller respectively. These indices are given by equation (23).

$$IAE = J_e = \sum_{k=1}^{N} |r_k - y_k|, \qquad ISU = J_u = \sum_{k=0}^{N} \left(u(k) - u_{ss}\right)^2 \tag{23}$$

The numerical values of IAE and ISU for both drivers applied in the RIP system are shown in Table 2.

**Table 2.** Indices performance obtained with linear and non-linear controller.

| | Arm Position *IAE* | Control Signal *ISU* | Computing Time (sec) |
|---|---|---|---|
| **Linear Controller** | 5.3218 x $10^4$ | 1.0644 x $10^3$ | 7.8215 |
| **Nonlinear Controller** | 4.8909 x $10^4$ | 570.6625 | 29.1743 |

The values in Table 2 show that the nonlinear PI controller has better performance in energy used, as in following references for positioning the arm. In the case of positioning the pendulum a linear PID controller was designed. So when acting linear PI controller in the arm RIP system, the IAE linear PID controller pendulum is 6.1272 x $10^3$, and when it acts nonlinear PI controller in the arm, the IAE linear PID controller pendulum is 2.9376 x $10^3$, which shows an improvement in the performance of the linear PID controller for the pendulum, when the nonlinear PI acts on the arm.

## 8. Conclusions

In this study, modeling, control and estimation of certain parameters of the inverted pendulum rotary experimentally, which has a satisfactory response we are performed. This model was used to design the PI and PID controllers for linear and nonlinear system. Of the assessment controllers shown that the performance of nonlinear PI control both reference tracking, and energy consumption is better than the linear PI control. Also, when the nonlinear PI controller acts on the arm of the system, the linear PID controller designed to position the pendulum vertically improves its efficiency. Although the computational time for the nonlinear controller is greater than the linear, a better result in energy

consumption and reference tracking is obtained. Future works aims to design a nonlinear for positioning the pendulum PID controller as well as using new control strategies for the RIP System.

**Acknowledgments**
The authors would like to acknowledge two important institutions in the development of this work: Universidad Politécnica Salesiana and Escuela Superior Politécnica del Litoral for all the support offered during the present study. Additionally, the authors are grateful with the GISCOR research who gave to the authors the facilities regarding the use of infrastructure and equipment.

**References**
[1] Sukontanakarn, Viroch; Parnichkun, Manukid; "Real-Time Optimal Control for Rotary Inverted Pendulum", American Journal of Applied Sciences 6 (6): 1106-1115, 2009 , ISSN 1546-9239
[2] J. Zhang and Y. Zhang, "Optimal linear modeling and its applications on swing-up and stabilization control for Rotary Inverted Pendulum," Control Conference (CCC), 2011 30th Chinese, Yantai, 2011, pp. 493-500.
[3] S. Jadlovská and J. Sarnovský, "A complex overview of the rotary single inverted pendulum system," ELEKTRO, 2012, Rajeck Teplice, 2012, pp. 305-310.doi: 10.1109/ELEKTRO.2012.6225609.
[4] P. Xue and W. Wei, "An Analysis on the Kinetic Model of a Rotary Inverted Pendulum, and Its Intelligent Control," Computational and Information Sciences (ICCIS), 2010 International Conference on, Chengdu, 2010, pp. 978-981
[5] K. Lai, J. Xiao, X. Hu, J. Fan and B. Wu, "Modeling and control for stability and rotation velocity of a rotary inverted pendulum," Industrial Electronics and Applications (ICIEA), 2015 IEEE 10th Conference on, Auckland, 2015, pp. 955-960.
[6] M. Roman, E. Bobasu and D. Sendrescu, "Modelling of the rotary inverted pendulum system," Automation, Quality and Testing, Robotics, 2008. AQTR 2008. IEEE International Conference on, Cluj-Napoca, 2008, pp. 141-146.
[7] Nguyen Duc Quyen; Ngo Van Thuyen; Nguyen Quang Hoc; Nguyen Duc Hien., "Rotary Inverted Pendulum and Control of Rotary Inverted Pendulum by Artificial Neural Network", Proc. Natl. Conf. Theor. Phys. 37 (2012), pp. 243-249.
[8] D. I. Barbosa, J. S. Castillo and L. F. Combita, "Rotary inverted pendulum with real time control," Robotics Symposium, 2011 IEEE IX Latin American and IEEE Colombian Conference on Automatic Control and Industry Applications (LARC), Bogota, 2011, pp. 1-6.
[9] Rahimi, A., Raahemifar, K., Kumar, K., Alighanbari, H. (2013). Controller design for rotary inverted pendulum system using particle swarm optimization algorithm. In Electrical and Computer Engineering (CCECE), vol., no., pp.1-5.
[10] Yunhai Hou., Hongwei Zhang., Kai Mei. (2011). Vertical-rotary inverted pendulum system based on fuzzy control. In Electrical and Control Engineering (ICECE), vol., no., pp.2804-2807.
[11] Barbosa, D.I., Castillo, J.S., Combita, L.F. (2011). Rotary inverted pendulum with real time control. In IEEE IX Latin American and IEEE Colombian, vol., no., pp.1-6.
[12] Hassanzadeh, I., Mobayen, S. (2008). GA based input-output feedback linearization controller for rotary inverted pendulum system. In Mechatronics and Its Applications, vol., no., pp.1-6.
[13] Cajo, R., Agila, W. (2015). Evaluation of Algorithms for Linear and Nonlinear PID Control for Twin Rotor MIMO System. In Computer Aided System Engineering (APCASE), vol., no., pp.214-219.